Published OnlineFirst January 11, 2007; DOI: 10.1158/1535-7163.MCT-06-0397

Characterization of a potent and selective small-molecule inhibitor of the PIM1 kinase

Sheldon Holder,[1,2,3] Marina Zemskova,[3] Chao Zhang,[4] Maryam Tabrizizad,[4] Ryan Bremer,[4] Jonathan W. Neidigh,[2] and Michael B. Lilly[1,2,3]

[1]Center for Molecular Biology and Gene Therapy, Departments of [2]Biochemistry and Microbiology and [3]Medicine, Loma Linda University School of Medicine, Loma Linda, California; and [4]Plexxikon, Inc., Berkeley, California

Abstract

The *pim-1* kinase is a true oncogene that has been implicated in the development of leukemias, lymphomas, and prostate cancer, and is the target of drug development programs. We have used experimental approaches to identify a selective, cell-permeable, small-molecule inhibitor of the *pim-1* kinase to foster basic and translational studies of the enzyme. We used an ELISA-based kinase assay to screen a diversity library of potential kinase inhibitors. The flavonol *quercetagetin* (3,3′,4′,5,6,7-hydroxyflavone) was identified as a moderately potent, ATP-competitive inhibitor (IC_{50}, 0.34 μmol/L). Resolution of the crystal structure of PIM1 in complex with quercetagetin or two other flavonoids revealed a spectrum of binding poses and hydrogen-bonding patterns in spite of strong similarity of the ligands. Quercetagetin was a highly selective inhibitor of PIM1 compared with PIM2 and seven other serine-threonine kinases. Quercetagetin was able to inhibit PIM1 activity in intact RWPE2 prostate cancer cells in a dose-dependent manner (ED_{50}, 5.5 μmol/L). RWPE2 cells treated with quercetagetin showed pronounced growth inhibition at inhibitor concentrations that blocked PIM1 kinase activity. Furthermore, the ability of quercetagetin to inhibit the growth of other prostate epithelial cell lines varied in proportion to their levels of PIM1 protein. Quercetagetin can function as a moderately potent and selective, cell-permeable inhibitor of the *pim-1* kinase, and may be useful for proof-of-concept studies to support the development of clinically useful PIM1 inhibitors. [Mol Cancer Ther 2007;6(1):163–72]

Received 7/10/06; revised 10/10/06; accepted 11/17/06.

Grant support: Department of Defense, Congressionally Directed Medical Research Program, Award W81XWH-04-1-0887.

The costs of publication of this article were defrayed in part by the payment of page charges. This article must therefore be hereby marked *advertisement* in accordance with 18 U.S.C. Section 1734 solely to indicate this fact.

Requests for reprints: Michael B. Lilly, Center for Molecular Biology and Gene Therapy, Loma Linda University School of Medicine, 11234 Anderson Street, Loma Linda, CA 92354. Phone: 909-558-8777; Fax: 909-558-0177. E-mail: mlilly@llu.edu

doi:10.1158/1535-7163.MCT-06-0397

Introduction

The *pim* family of serine-threonine kinases is composed of three highly homologous genes, *pim-1*, *pim-2*, and *pim-3*. These enzymes are increasingly being recognized as important mediators of survival signals in cancers, stress responses, and neural development (1–6). In addition, these kinases are constitutively expressed in some tumors and function as true oncogenes. Thus, they are of significant interest as targets for therapeutic intervention.

Small-molecule inhibitors are important molecular probes for studying protein kinases. In addition, they may serve as protype therapeutic agents for treating diseases resulting from unregulated kinase activity. Three prior reports have shown that known, promiscuous kinase inhibitors can inhibit PIM1 function *in vitro*. Jacobs et al. (7) showed that several staurosporine and bisindoyl-maleimide analogues, as well as the morpholino-substituted chromone LY294002, were able to inhibit PIM1 activity *in vitro*. Subsequently, Fabian et al. (8) presented an interaction map involving 113 kinases and 20 small-molecule kinase inhibitors now under clinical study. Only three inhibitors had detectable binding to (and presumably inhibitory activity against) PIM1—two staurosporine analogues and flavopiridol, a flavonoid undergoing evaluation as an inhibitor of cyclin-dependent kinases. A recent report (9) confirmed the activity of bisindoylmaleimide derivatives as well as some flavonoids *in vitro*. All of the identified inhibitors either lacked specificity for PIM1 or were only modestly active at low micromolar concentrations, or both. Furthermore, none of these reports showed that the test agents could selectively inhibit PIM1 activity in intact cells.

To further our basic and translational studies of the *pim* kinases, we have sought to identify small-molecule inhibitors of PIM1. We here report that the flavonol *quercetagetin* is a selective PIM1 inhibitor with nanomolar potency and can differentially inhibit the kinase in cell-based assays.

Materials and Methods

Cell Lines and Culture Methods

The prostate epithelial cell lines RWPE1, RWPE2, LNCaP, and PC3 were obtained from the American Type Culture Collection (Manassas, VA) and cultured in the recommended medium. We produced additional pools of RWPE2 prostate cells that overexpressed *pim-1* through retroviral transduction. The coding region for the human *pim-1* gene was cloned into the pLNCX retroviral vector (Clontech, Mountain View, CA). Infectious viruses were produced in the GP-293 packaging cell line by cotransfection with retroviral backbone plasmids (pLNCX or pLNCX/*pim-1*) and with pVSV-G, a plasmid that expresses the envelope

Published OnlineFirst January 11, 2007; DOI: 10.1158/1535-7163.MCT-06-0397

glycoprotein from vesicular stomatitis virus. Forty-eight hours after transfection, the medium was collected and the virus particles were concentrated as described in the manufacturer's protocol (Clontech). RWPE2 cells were plated at 1×10^5 per 60-mm plate 16 to 18 h before infection. Cells were infected with 5×10^4 viral particles in the presence of 8 μg/mL polybrene. After 6 h of incubation, the virus-containing medium was replaced with fresh medium, and on the next day G418 (400 μg/mL) was added to select infected cells. After 10 days of selection, stable cell pools were established and PIM1 expression was verified by immunoblotting.

For growth-inhibition experiments, cells were plated onto 24-well plates and fixed with formaldehyde at intervals. Cell number was quantified by crystal violet staining (10).

Recombinant *pim* Kinases and Kinase Assays

We prepared recombinant PIM1 and PIM2 as glutathione *S*-transferase (GST) fusions in *Escherichia coli*, as described (11). For the inhibitor screening assays, a solid-phase kinase assay was developed based on our demonstration that PIM1 is a potent kinase for phosphorylating BAD on Ser^{112} (11, 12). Ninety-six-well flat-bottomed plates were coated overnight at 4°C with recombinant GST-BAD [1 μg/well in HEPES buffer: 136 mmol/L NaCl, 2.6 mmol/L KCl, and 20 mmol/L HEPES (pH 7.5)]. The plates were then blocked for 1 h at room temperature with 10 μg/mL bovine serum albumin in HEPES buffer. The blocking solution was then removed and 5 μL of each inhibitor, dissolved in 50% DMSO, were added to each well. Then, 100 μL of kinase buffer [20 mmol/L MOPS (pH 7.0), 12.5 mmol/L $MgCl_2$, 1 mmol/L $MnCl_2$, 1 mmol/L EGTA, 150 mmol/L NaCl, 10 μmol/L ATP, 1 mmol/L DTT, and 5 mmol/L β-glycerophosphate] containing 25 ng recombinant GST-PIM1 kinase were added to each well. The final concentration of each inhibitor was ~10 μmol/L. The plate was placed on a gel slab dryer prewarmed to 30°C, and the kinase reaction was allowed to proceed. The reaction was stopped after 60 min by removal of the reaction buffer, followed by the addition of 100 μL of HEPES buffer containing 20 mmol/L EDTA to each well. Phosphorylated GST-BAD was detected by an ELISA reaction, using as first antibody a monoclonal anti–phospho-BAD(S112) antibody (Cell Signaling, Danvers, MA), a secondary goat anti-mouse IgG-peroxidase conjugated antibody (Pierce, Rockford, IL), and Turbo-TMB peroxidase substrate (Pierce). The level of phosphorylated GST-BAD present was proportional to the absorbance at 450 nm.

For quantitative and kinetic studies of inhibitors against various BAD(S112) kinases, a solution phase assay was used. A biotinylated peptide based on the PIM1 phosphorylation site of human BAD was synthesized (GGAGAVEIRSRHSSYPAGTE) and used as the assay substrate. Recombinant GST-PIM1 (25 ng/reaction) was preincubated with various concentrations of inhibitors in the previous kinase buffer (final volume 100 μL). The reaction proceeded by addition of substrate peptide, followed by incubation for 5 min in a 30°C water bath. The reaction was terminated by transferring the mixture to a streptavidin-coated 96-well plate (Pierce) containing 100 μL/well of 40 mmol/L EDTA. The biotinylated peptide substrate was allowed to bind to the plate at room temperature for 10 min. The level of phosphorylation was then determined by ELISA as described above. Curve fitting and enzyme analyses were done using GraphPad Prism version 4.00 for Windows (GraphPad Software, San Diego, CA). For the additional BAD(S112) kinases [PIM2, RSK2 (ribosomal S6 kinase 2), and PKA (cyclic AMP–dependent protein kinase)], reaction components were as described above. As with the PIM1 assays, an ATP concentration of 10 μmol/L was used. Furthermore, with each kinase, linear reaction velocities for the duration of the reaction were confirmed (data not shown).

To further assess the specificity of quercetagetin as a PIM1 inhibitor, its activity against a panel of serine-threonine kinases was also studied through a commercial kinase inhibitor profiling service (KinaseProfiler; Upstate Biotechnology, Charlottesville, VA). All KinaseProfiler assays were conducted using 10 μmol/L ATP concentrations.

Small-Molecule Library Screening

We obtained a library of 1,200 compounds that had structural affinity to known kinase inhibitors (TimTec, Inc., Newark, DE). The entire library was screened once with our solid-phase ELISA kinase assay, with each compound at ~10 μmol/L concentration. Positive hits were rescreened at the same concentration. Compounds that had reproducible activity at 10 μmol/L were then screened at a range of concentrations from 0.001 to 300 μmol/L. Additional flavonoids were purchased from Indofine Chemicals (Hillsborough, NJ) and were tested in a similar protocol.

Measurement of PIM1 Kinase Activity in Cells

RWPE2 cell pools, stably infected with empty retrovirus or *pim-1*–encoding retrovirus, were seeded in six-well plates at 5×10^5 cells per well. After 18 h, the normal supplemented keratinocyte medium was removed and replaced with supplement-free keratinocyte medium. Cells were then incubated for an additional 20 h. Quercetagetin, or an equivalent volume of DMSO, was added to the cells 3 h before the end of the starvation period. At the conclusion of the starvation period, the cells were washed twice with PBS and subsequently lysed in a denaturing buffer with protease, phosphatase inhibitors. The lysates were normalized by total protein content (BCA protein assay, Pierce), then analyzed by immunoblotting with the following antibodies: monoclonal anti-PIM1 (Santa Cruz Biotechnologies, Santa Cruz, CA); monoclonal anti–β-actin (Sigma, St. Louis, MO); monoclonal anti-BAD (Transduction Laboratories, Franklin Lakes, NJ); and monoclonal anti–phospho-BAD(S112), polyclonal anti–phospho-AKT(S473), and anti-AKT (all from Cell Signaling).

Cloning, Expression, Purification, and Crystallization of PIM1

The production, purification, and characterization of recombinant 6His-tagged PIM1 proteins for crystallography have been described previously (13). To obtain cocrystals of complexes of the protein with ligands, the protein solution was initially mixed with the compound (dissolved

in DMSO) at a final compound concentration of 1 mmol/L and then set up for crystallization. The protein was crystallized by a sitting-drop, vapor-diffusion experiment in which equal volumes of protein (10–15 mg/mL concentration) and reservoir solution [0.4–0.9 mol/L sodium acetate, 0.1 mol/L imidazole (pH 6.5)] were mixed and allowed to equilibrate against the reservoir at 4°C. The crystals routinely grew to a size of 200 × 200 × 800 μm in ~2 to 3 days.

Structure Determination

X-ray diffraction data were collected at Advanced Light Source (Berkeley, CA). All data were processed and reduced with MOSFLM and scaled with SCALA of the CCP4 suite of programs using the software ELVES. The space group of all crystals was determined to be $P6_5$, with the cell axes being approximately 99, 99, and 80, and one protein monomer being present in the asymmetrical unit. All structures were determined by molecular replacement using the apo PIM1 structure (1YWV; ref. 13) as a model, and refined by CNX and REFMAC5. Crystallographic statistics are reported in Supplementary Table S1.[5] The coordinates and structure factors for the structures have been deposited with the RCSB Protein Data Bank (accession codes 2O63, 2O64, 2O65).

Results

Screening of a Chemical Library with Structural Affinity to Known Kinase Inhibitors

As an initial approach to the identification of PIM1 inhibitors, we screened a library of small molecules whose structures were similar to those of known kinase inhibitors. Of the seven compounds that had reproducible inhibitory activity at 10 μmol/L, six were flavonoids [quercetin, luteolin, kaempferol, 7-hydroxyflavone, (*S*)-5,7-dihydroxy-8-(3-methylbut-2-ene)flavanone, and (*R*)-5,7-dihydroxyflavanone]. These compounds exhibited a range of inhibitory potencies (as IC_{50}) from 1.1 to 60 μmol/L. Thirty-seven other flavonoids failed to show detectable inhibitory activity at 10 μmol/L. These inactive compounds were characterized in most cases by bulky (charged or uncharged) groups at the 3, 3′, 4′, or 7 positions; lack of at least two hydrogen bond donors on the A or C rings; presence of glycoside linkages; or failure of all rings to adopt a planar conformation.

The most active compound in the chemical library was the flavonol quercetin (IC_{50}, 1.1 μmol/L), a known inhibitor of kinases and many other enzymes (14–19). Furthermore, six of the seven compounds with reproducible activity at 10 μmol/L were flavonoids. Hence, we screened additional flavonoids to identify molecules with inhibitory activity against the PIM1 kinase (Fig. 1). The most active molecule was the flavonol *quercetagetin* (IC_{50}, 0.34 μmol/L). The four flavonoids with the highest inhibitory activity were characterized by the presence of five to six –OH groups distributed between the A and B rings. In comparison, the hydroxyl groups on the B ring seemed to be more critical for the activity of the compounds than those on the A ring, as compounds with an unsubstituted B ring showed greatly reduced activity. Finally, a hydrophobic substituent at the 8 position was tolerated.

Quercetagetin Is a Selective, Potent Inhibitor of PIM1 *In vitro*

To assess the selectivity of quercetagetin for PIM1, we determined its IC_{50} value toward the alternative BAD(S112) kinases RSK2, PKA, and PIM2 (Table 1). The IC_{50} of quercetagetin for PIM1 kinase was 0.34 μmol/L, whereas the corresponding values for the other kinases were 9- to 70-fold higher.

To further characterize the specificity of quercetagetin, its inhibitory activity was examined at 1 or 10 μmol/L against additional serine-threonine kinases (c-Jun-NH_2-kinase 1, PKA, Aurora-A, c-RAF, and PKCθ; Fig. 2). At the lower concentration, the selectivity of quercetagetin was most apparent. In the presence of 1 μmol/L inhibitor, PIM1 activity was inhibited by 92%. In contrast, the activity of the other kinases was inhibited by only 0% to 41%. In aggregate, these studies established that quercetagetin was a severalfold more potent inhibitor for *pim-1* kinase than for seven other serine-threonine kinases. In addition, quercetagetin was completely inactive against the *c-abl* tyrosine kinase when tested at the 200 μmol/L concentration (data not shown).

Crystallographic Analysis of Quercetagetin in Complex with PIM1

Recently, several crystal structures of the PIM1 kinase have been solved and presented, including apo forms and the enzyme in complex with a variety of ligands (7, 9, 13, 20, 21). Because the PIM1 protein has several unique structural features around its ATP-binding pocket, including the lack of the canonical hydrogen bond donor from the hinge region typically used by kinases to bind ATP-like ligands, we determined the crystal structure for the kinase in complex with three flavonoid inhibitors: quercetagetin, myricetin, and 5,7,3′,4′,5′-pentahydroxyflavone (Fig. 3).

The three flavonoid inhibitors show two distinct binding poses, denoted here as orientations I and II, respectively. Quercetagetin, the compound with two hydroxyl groups on the B ring, adopts orientation I, whereas the compounds with a trisubstituted B ring (myricetin and 5,7,3′,4′,5′-pentahydroxyflavone) adopt orientation II.

The binding pose of quercetagetin in PIM1 (Fig. 3A) closely resembles that of quercetin in phosphatidylinositol 3-kinase γ (1E8W; ref. 22) and that of fisetin in CDK6 (1XO2; ref. 23), designated here as orientation I. As seen in the two earlier structures (Fig. 3D and E), the 3-OH of the quercetagetin (Fig. 3A) makes a canonical hydrogen bond with backbone carbonyl oxygen of the hinge residue Glu^{121}. In addition, the B ring of quercetagetin binds deep inside the PIM1 ATP-binding pocket, with the 4′-hydroxyl group hydrogen-bonded to the side chains of two highly conserved residues, Lys^{67} and Glu^{89}. However, significant differences were also observed between the current

[5] Supplementary data for this article are available at Molecular Cancer Therapeutics Online (http://mct.aacrjournals.org/).

Published OnlineFirst January 11, 2007; DOI: 10.1158/1535-7163.MCT-06-0397

structure and the two reported structures. In both 1E8W and 1XO2, the 4-keto group of the chromenone core of the compound formed a hydrogen bond with the same hinge amide nitrogen [Val^{882} in phosphatidylinositol 3-kinase γ (Fig. 3D) and Val^{101} in CDK6 (Fig. 3E)]. However, there is no direct interaction between the 4-keto group of quercetagetin and the amide nitrogen of the corresponding residue Pro^{123} in PIM1 because proline is incapable of acting as a hydrogen bond donor. Instead, the 4-keto group of quercetagetin makes close contact with the backbone Cα of Arg^{122} (3.4 Å). It is not clear whether this interaction makes a positive contribution to the binding of quercetagetin to PIM1.

The B ring of quercetagetin binds deep inside the PIM1 ATP-binding pocket. The 4′-hydroxyl group forms hydrogen bonds with both Lys^{67} and Glu^{89}, two of the most conserved residues in kinases. As has been noted, satisfying the hydrogen bonding requirements at this region is one of the determining features of binding of compounds to PIM1 (13).

When compared with quercetagetin, the chromenone core of myricetin (Fig. 3B) and 5,7,3′,4′,5′-pentahydroxyfavone (Fig. 3C) has flipped 180° in PIM1 such that the B ring is now oriented toward the entrance of the ATP pocket. A possible explanation for adopting this orientation is that the interior of the ATP pocket cannot accommodate the B ring with three hydroxyl substitutions. Although they bind in the same orientation, there are important differences between the binding poses of the two compounds, which can be attributed to the presence or absence of the 3-hydroxyl group. The 3-hydroxyl group in myricetin still makes a hydrogen bond with the carbonyl oxygen of Glu^{121}, despite the difference in binding orientation. Because of the adjacent 4-keto group, the 3-hydroxyl is likely to be most acidic of all the hydroxyl groups in the compound, and, as a result, it dictates the overall positioning of the compound. Another interaction that may contribute to the observed binding pose is a hydrogen bond between the 3′-hydroxyl group of myricetin and the carbonyl oxygen of Pro^{123} (Fig. 3B). The importance of the 3-hydroxyl group is evident. The second compound, 5,7,3′,4′,5′-pentahydroxyflavone, lacking such a group, makes no direct interaction with the hinge region.

Quercetagetin Inhibits PIM1 Kinase Activity in Intact Cells

To determine if quercetagetin could act as a cell-permeable PIM1 inhibitor, we examined the activity of the flavonol in RWPE2 prostate cancer cells. We studied the phosphorylation of endogenous BAD on Ser^{112}, under conditions of growth factor starvation, as an indicator of intracellular PIM1 activity (Fig. 4).

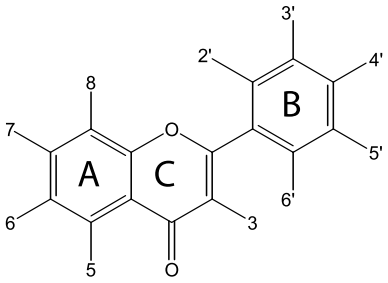

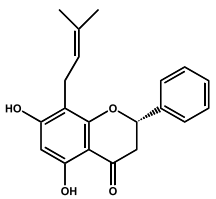

(S)-5,7-dihydroxy-8-(3-methylbut-2-ene)flavanone

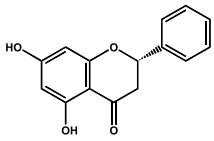

(S)-5,7-dihydroxyflavanone

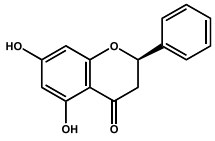

(R)-5,7-dihydroxyflavanone

Flavonoid	3	5	6	7	8	2'	3'	4'	5'	6'	IC_{50} (μM)
quercetagetin	OH	OH	OH	OH	H	H	OH	OH	H	H	0.34
gossypetin	OH	OH	H	OH	OH	H	OH	OH	H	H	0.43
5,7,3',4',5'-pentahydroxyflavone	H	OH	H	OH	H	H	OH	OH	OH	H	0.65
myricetin	OH	OH	H	OH	H	H	OH	OH	OH	H	0.78
fisetin	OH	H	H	OH	H	H	OH	OH	H	H	0.85
apigenin	H	OH	H	OH	H	H	H	OH	H	H	0.94
3,7,4'-trihydroxyflavone	OH	H	H	OH	H	H	H	OH	H	H	0.98
quercetin	OH	OH	H	OH	H	H	OH	OH	H	H	1.1
kaempferol	OH	OH	H	OH	H	H	H	OH	H	H	1.3
luteolin	H	OH	H	OH	H	H	OH	OH	H	H	1.6
morin	OH	OH	H	OH	H	OH	H	OH	H	H	2.7
7,3'-dihydroxyflavone	H	H	H	OH	H	H	OH	H	H	H	4.52
3,7-dihydroxyflavone	OH	H	H	OH	H	H	H	H	H	H	4.6
7,3',4',5'-tetrahydroxyflavone	H	H	H	OH	H	H	OH	OH	OH	H	7.8
3,6,2',4'-tetrahydroxyflavone	OH	H	OH	H	H	OH	H	OH	H	H	8.3
(S)-5,7-dihydroxy-8-(3-methylbut-2-ene)flavanone	see illustration above										12.5
7-hydroxyflavone	H	H	H	OH	H	H	H	H	H	H	14
5,7-dihydroxyflavone	H	OH	H	OH	H	H	H	H	H	H	15
7,8,4'-trihydroxyflavone	H	H	H	OH	OH	H	H	OH	H	H	22
(R)-5,7-dihydroxyflavanone	see illustration above										60.2
(S)-5,7-dihydroxyflavanone	see illustration above										107

Figure 1. Identification of flavonoids with PIM1 inhibitory activity. Structures of all studied flavonoids with detectable PIM1 inhibitory activity, given with their IC_{50} values.

Table 1. Quercetagetin is a selective inhibitor of the PIM1 kinase over other BAD(S112) kinases

Kinase	IC_{50} (μmol/L)	Log IC_{50} (μmol/L)	SE of log IC_{50}	R^2
PIM1	0.34	−0.46	0.12	0.98
PIM2	3.45	0.55	0.22	0.94
PKA	21.2	1.33	0.23	0.94
RSK2	2.82	0.45	0.09	0.99

NOTE: All data were derived from nonlinear regression analyses using a three-parameter logistic that assumes a Hill coefficient of −1.

RWPE2 cells infected with a *neo*-expressing retrovirus showed little phospho-BAD(S112) when cultured overnight in basal serum-free medium. However, cells with enforced expression of PIM1 kinase had a 4-fold higher amount of phospho-BAD, reflecting the ability of the PIM1 protein to phosphorylate the endogenous BAD protein. When *pim-1*–expressing cells were treated with quercetagetin, phospho-BAD(S112) levels were markedly reduced in proportion to the concentration of the inhibitor. Half-maximal inhibition occurred at 5.5 μmol/L extracellular concentration. Quercetagetin did not inhibit the activity of the AKT kinase under these conditions, as indicated by persistent phosphorylation of AKT on Ser^{473}. These data indicate that quercetagetin was able to selectively block the ability of PIM1 to phosphorylate BAD in intact cells.

Quercetagetin Treatment Reproduces a Known *pim-1* Knockdown Phenotype

If quercetagetin acts as a true PIM1 inhibitor, then it should reproduce a *pim-1*–dependent phenotype in the target cells. We have shown that PIM1 inhibition by genetic means (small interfering RNA) inhibits the proliferation of RWPE1 and RWPE2 cells (Supplementary Fig. S1).[5] We therefore determined if quercetagetin could reproduce this phenotype. RWPE2 cells were treated with quercetagetin for up to 72 h (Fig. 5A). Marked dose-dependent growth inhibition was apparent by 24 h, leading to persistent growth arrest thereafter. Quercetagetin reproduced this *pim-1*–dependent phenotype at a drug concentration that inhibited the enzyme in cells (ED_{50}, 3.8 μmol/L; Fig. 5B). Similar results were seen in RWPE1 cells (data not shown). Apoptotic cells, showing cytoplasmic blebbing and detachment, were rare, but dividing cells virtually disappeared in cultures treated with quercetagetin at 6.25 μmol/L or higher concentrations (data not shown). DNA histograms obtained at 24 h after the addition of quercetagetin (6.25 μmol/L) or DMSO vehicle were very similar (Fig. 5C). Neither showed a <2n population suggestive of apoptosis. There was a slight increase in the proportion of cycling cells ($S + G_2$-M) in the drug-treated samples.

A PIM1 inhibitor would be predicted to inhibit the growth of cells that express the molecular target, more than cells with little or no *pim-1* expression. We examined the effects of quercetagetin on the growth of prostate cell lines that express a spectrum of PIM1 levels. RWPE2 cells expressed the highest amount of PIM1 protein; PC3 had an intermediate level; and LNCaP cells showed the lowest amount of kinase protein (Fig. 6A). Treatment of the cells with various concentrations of quercetagetin for 72 h resulted in inhibition of cell growth (Fig. 6B). At all concentrations, RWPE2 cells were inhibited the most, being significantly more sensitive to quercetagetin growth inhibition than the other prostate cancer cell lines. PC3 cells showed intermediate growth suppression and were also significantly more sensitive than were LNCaP cells at quercetagetin concentrations of ≤12.5 μmol/L. Thus, the ability of the flavonol to inhibit proliferation was proportional to the amount of PIM1 protein in the target cells, particularly at lower drug concentrations. Although other interpretations are possible, these data support our observation that quercetagetin can act as a PIM1 inhibitor.

Discussion

The development of clinically useful small-molecule kinase inhibitors has been a seminal event in the world of oncology. Flavonoids were among the early scaffold structures identified as potential kinase inhibitors. However, although many flavones, isoflavones, and flavonols have been shown to regulate the activity of kinases in cell-based assays, fewer data exist to show that these molecules can directly bind and inhibit kinase targets both *in vitro* and in cells. It is clear that some flavonoids are ATP-competitive ligands for both tyrosine and serine-threonine kinases, as well as other ATP-binding enzymes. The flavonol quercetin is one such ligand, and its ability to directly bind to ATP-binding enzymes has been well shown. At low-micromolar concentrations, it directly binds and inhibits such diverse enzymes as the phosphatidylinositol 3-kinase (14), the epidermal growth factor receptor tyrosine kinase (15), retroviral reverse transcriptases (16), DNA gyrases (17), phosphodiesterases (18), and thioredoxin reductase (19). Other direct flavonoid inhibitors have been described for RSK2 kinase (24), mitogen-activated protein/extracellular signal-regulated kinase 1 (25), and several cyclin-dependent kinases (23, 26–28). One such ligand, flavopiridol, has already entered clinical trials for the treatment of cancer. Others, such as PD98059, are familiar laboratory reagents for inhibition of kinase pathways. We now show, by means of crystallography, that quercetagetin is a direct ligand for the ATP-binding pocket of PIM1 kinase (Fig. 3).

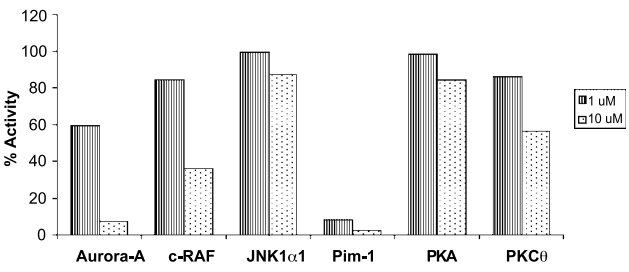

Figure 2. Quercetagetin is a selective inhibitor of PIM1 kinase. Inhibitor activity of quercetagetin at 1 and 10 μmol/L final concentration against a spectrum of serine-threonine kinases of a panel of kinases, assessed by KinaseProfiler assay. The activity in the presence of vehicle only was taken to be 100% activity. *Columns*, mean of duplicate determinations.

Published OnlineFirst January 11, 2007; DOI: 10.1158/1535-7163.MCT-06-0397

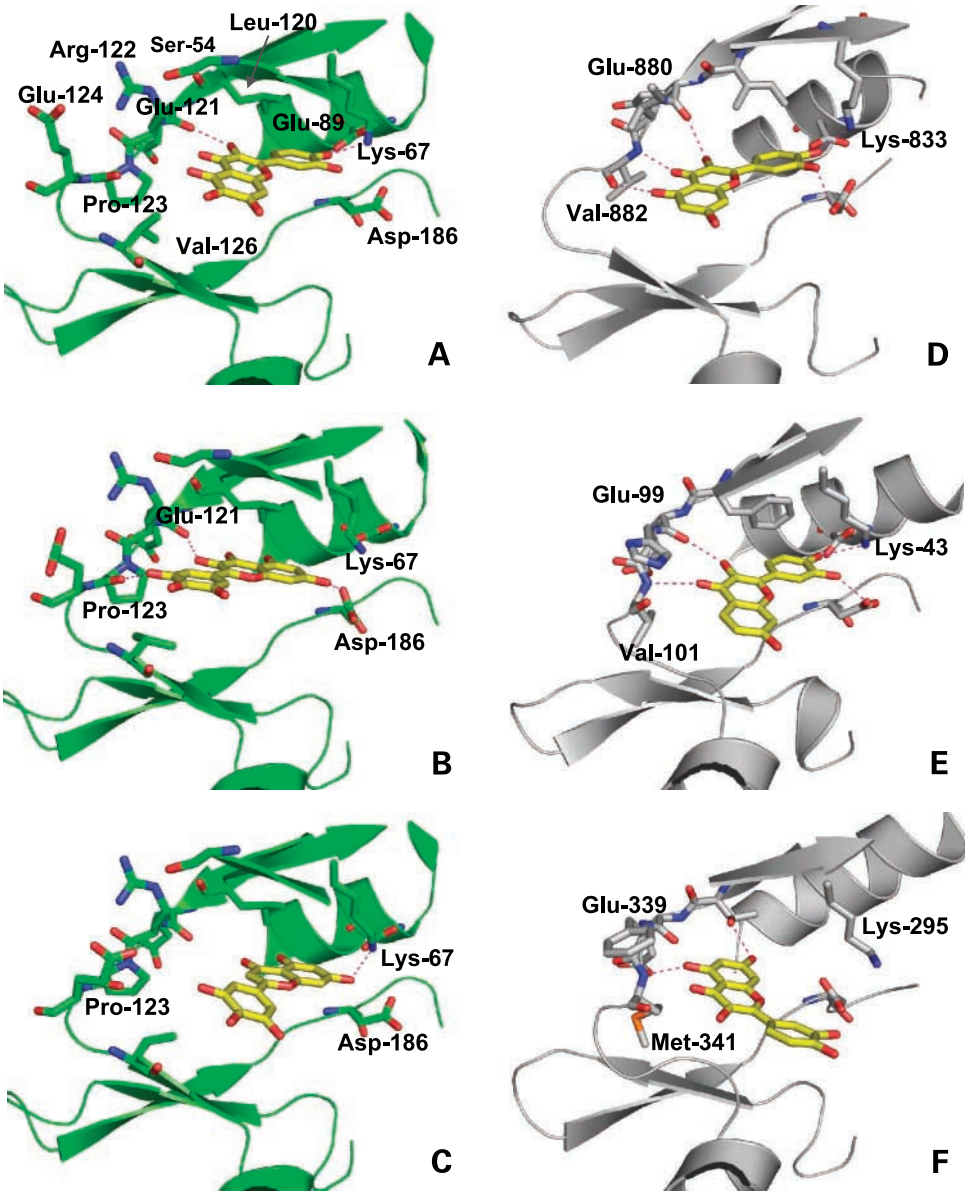

Figure 3. X-ray crystal structures of flavonoids bound to the ATP-binding sites of PIM1 and comparison with structures of flavonoids in complex with other kinases. Of the three compounds cocrystallized with PIM1, quercetagetin (**A**) orients the B ring inside the pocket (orientation I), whereas both myricetin (**B**) and 5,7,3′,4′,5′-pentahydroxyflavone (**C**) flip the B ring out toward solvent (orientation II). Both binding orientations have been observed in the crystal structures of flavonoids bound to other kinases. 1E8W (**D,** quercetin in complex with phosphatidylinositol 3-kinase γ) and 1XO2 (**E,** fisetin in complex with CDK6) represent orientation I, whereas 2HCK (**F,** quercetin in complex with HCK) exemplifies orientation II. All pictures show residues that form hydrogen bond with the inhibitors (Lys^{67}, Glu^{89}, Glu^{121}, and Asp^{186}). In the PIM1 structures, the three residues near the ATP-binding site that differentiate PIM1 from PIM2 (Ser^{54}, Glu^{124}, and Val^{126}) are also shown. The inhibitors are colored by atom type: *red,* oxygen atoms; *yellow,* carbon atoms. *Dashed purple lines,* hydrogen bonds.

Specificity is always a concern with ATP pocket ligands. There are probably no absolutely selective inhibitors for a kinase but rather ligands that show a spectrum of affinities for their various targets. We have shown that quercetagetin is severalfold more active against PIM1 than against eight other serine-threonine kinases and a tyrosine kinase, either with *in vitro* assays or in cell cultures. Interestingly, quercetagetin showed 10-fold more selectivity for PIM1 than for the homologous PIM2 kinase (sequence identity 56%). The ATP-binding pockets of these two kinases are identical with the exception of three residues along the edge of the PIM1 ATP-binding pocket—Ser^{54} (Ala^{58} in PIM2), Glu^{124} (Leu^{120} in PIM2), and Val^{126} (Ala^{122} in PIM2). Val^{126} of PIM1 makes direct van der Waal's contact with the A ring of quercetagetin (Fig. 3A). Loss of such a contact due to the Val-to-Ala substitution is likely a contributing factor to the reduced activity of the compound in PIM2. The other residues are located close to the hinge Arg^{122} (Arg^{118} in PIM2). The polar side chains of Ser^{54} and Glu^{124} can form hydrogen bonds with Arg^{122}, thus affecting its conformation. Substitutions of these residues to hydrophobic amino acids in PIM2 will change the local environment (Fig. 3A).

The only large-scale examination of the specificity of flavonoid kinase inhibitors was reported recently by Fabian et al. (8). This investigation used a competitive binding assay to predict the inhibitor potency and specificity of the test agents. Flavopiridol was tested for binding affinity to 119 kinases. Twenty-three kinases bound flavopiridol under the test conditions, with binding constants ranging from 0.019 to 6.6 μmol/L. Interestingly, the tested cyclin-dependent

Published OnlineFirst January 11, 2007; DOI: 10.1158/1535-7163.MCT-06-0397

kinases bound flavopiridol less well than did calcium/calmodulin–dependent protein kinase kinase I. These data suggest that cyclin-dependent kinases may not be the only kinases inhibited in cells by flavopiridol. Both PIM1 and PIM2 were among the bound kinases, with binding constants of 0.52 and 0.65 μmol/L, respectively. Although there is no absolute correlation between binding constants and enzymatic activity, flavopiridol could conceivably inhibit the activity of both PIM1 and PIM2 in test systems. Because quercetagetin has not been tested against a large number of other kinases, we cannot predict what other enzymes would be perturbed by this flavonoid. It is likely, however, that its spectrum of selectivity will be substantially different from that of flavopiridol. Quercetagetin showed clear preference for inhibiting PIM1 over PIM2, whereas flavopiridol did not. Furthermore quercetagetin inhibited the activity of the Aurora-A kinase (IC_{50}, ~4 μmol/L), a kinase that did not bind flavopiridol (8). The substantial

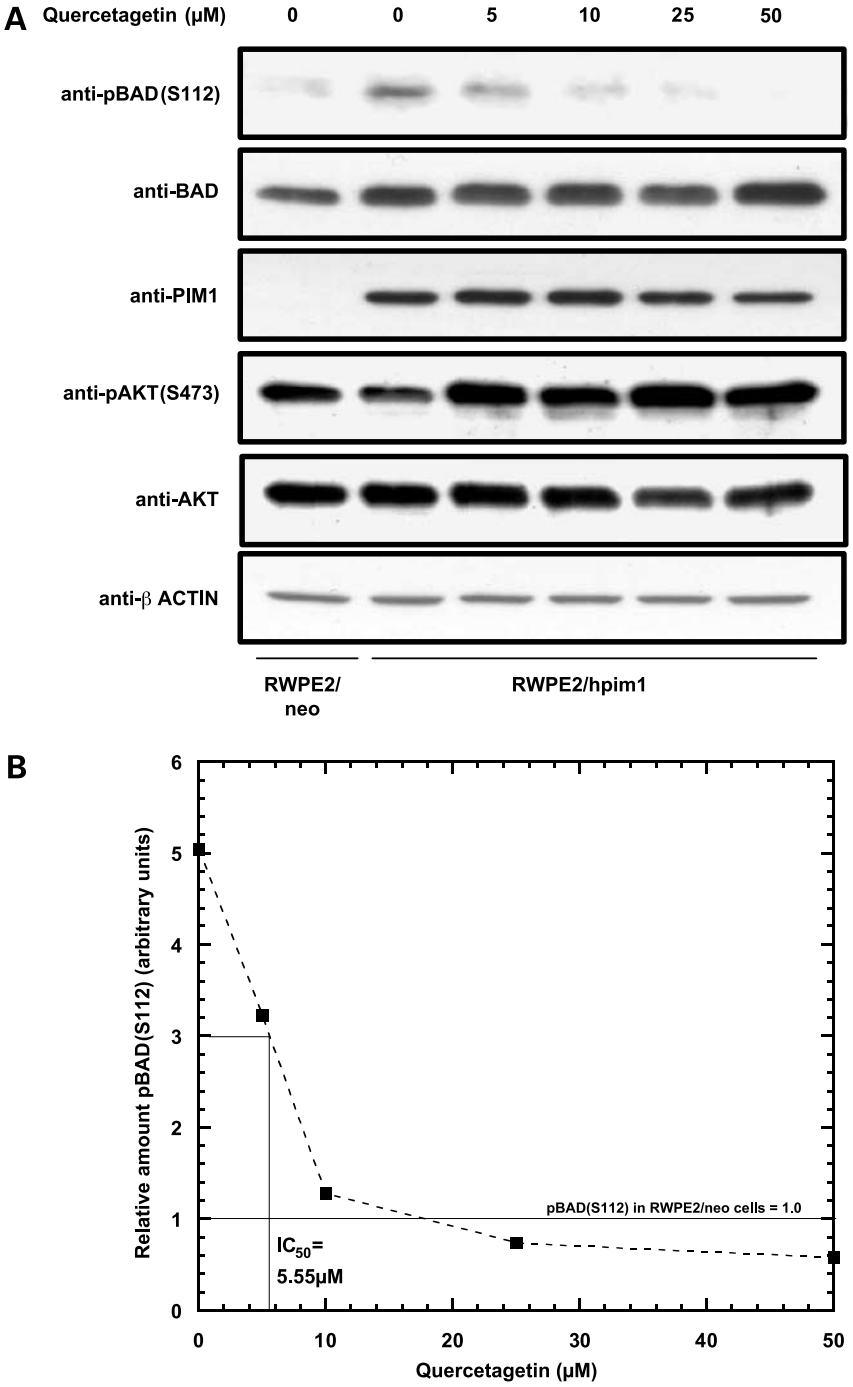

Figure 4. Quercetagetin inhibits PIM1 kinase activity in intact cells. **A,** RWPE2/neo or RWPE2/hpim1 cells were cultured in unsupplemented keratinocyte medium overnight, then treated with quercetagetin (0–50 μmol/L) for 3 h. Lysates were then prepared and examined by immunoblotting with the indicated antibodies. **B,** quantitation of the pBAD(S112)/actin ratio in immunoblots by using densitometry on the digital file. ED_{50}, 5.55 μmol/L.

Published OnlineFirst January 11, 2007; DOI: 10.1158/1535-7163.MCT-06-0397

homology between Aurora-A kinase and PIM1 kinase likely contributed to the low-level inhibitory activity of quercetagetin for the former; Aurora-A and PIM1 are 29% identical over their entire kinase domains; and the ATP binding pockets have 68% conserved amino acids.

An earlier, smaller-scale study looked at the effect of the flavonol quercetin on the *in vitro* kinase activity of 25 kinases, none of which were *pim* family kinases (29). At the tested concentration (20 μmol/L), quercetin inhibited the enzymatic activity of eight of the kinases. The propensity of this flavonol to form aggregates in aqueous solution has been advanced as an explanation for its widespread enzyme-inhibitory activity *in vitro* (30). We have not detected quercetagetin aggregates at concentrations of <10 μmol/L in aqueous solution, using a light-scattering assay (data not shown). Thus, we feel that this artifact does not account for the ability of this flavonol to inhibit PIM1 at nanomolar concentrations.

Because of the potential ambiguities that may accompany the use of small-molecule kinase inhibitors, a series of standards have been proposed for their use (29). To validate the results, it is desirable to show that the effects of an inhibitor disappear when a drug-resistant mutant of the protein kinase is overexpressed. Although convincing, this standard often fails due to the lack of an identified mutant with the desired properties. No such mutant has been identified for any of the *pim* kinases. Another potential standard is to show that the cellular effect of the drug occurs at the same concentrations that prevents the phosphorylation of an authentic physiologic substrate of the protein kinase. We have seen in these studies that half-maximal growth inhibition of prostate cancer cells occurred at a drug concentration (3.8 μmol/L) that approximated the IC_{50} for PIM1 enzyme inhibition in cells (5.5 μmol/L). Furthermore, the selectivity for prostate cancer growth inhibition, in proportion to endogenous PIM1 levels, was greatest at 6.25 μmol/L. Higher concentrations suppressed growth more, but the relationship to endogenous PIM1 levels was obscured. These data suggest that, at relatively low concentrations (perhaps 5–10 μmol/L), the growth-inhibitory effects of quercetagetin likely involve PIM1 antagonism. A third standard is to observe the same effect with at least two structurally unrelated inhibitors of the protein kinase. Previously described inhibitors of *pim*

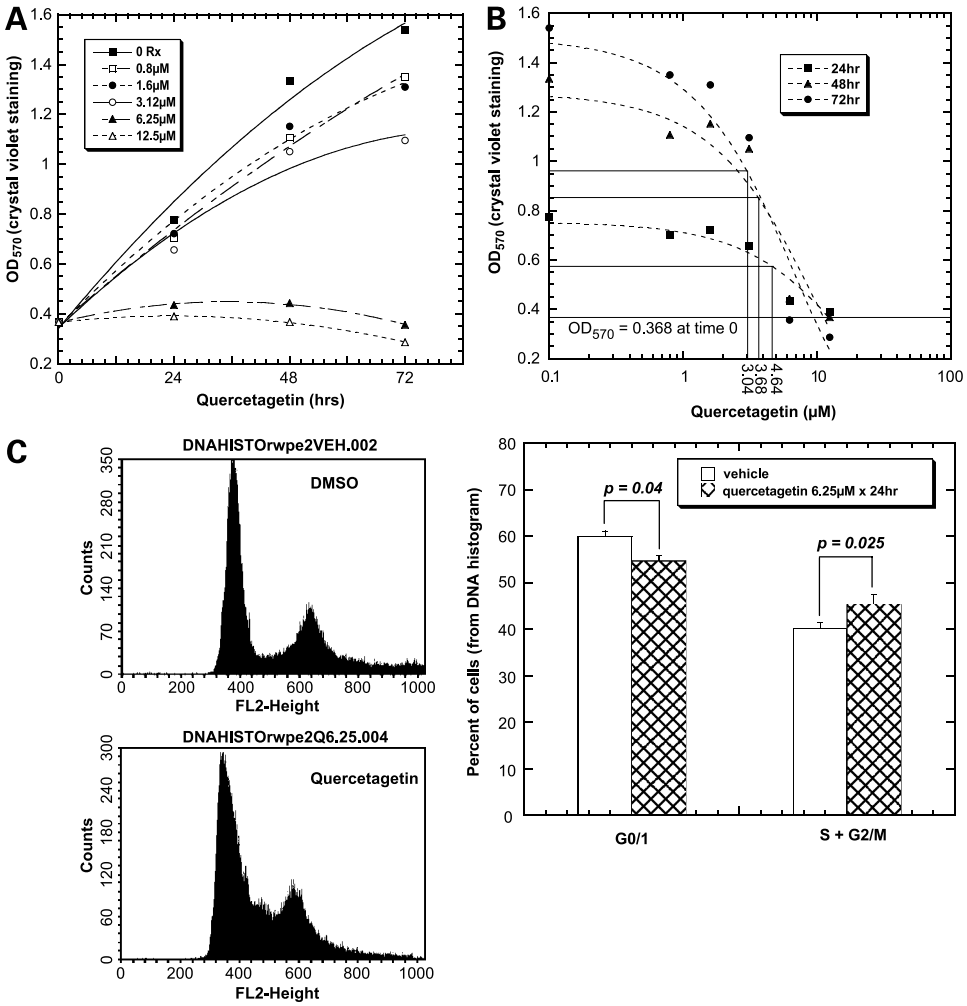

Figure 5. Quercetagetin inhibits growth of prostate cancer cells at concentrations that inhibit PIM1 kinase activity. **A,** growth curve of RWPE2 cells with different concentrations of quercetagetin. Cell number is measured by crystal violet staining. *Points,* mean of triplicate determinations from one of four similar experiments. **B,** calculation of ED_{50} at 24, 48, and 72 h of drug exposure. Average ED_{50} from all curves is 3.8 μmol/L. **C,** DNA histograms from RWPE2 cells treated with vehicle or quercetagetin 6.25 μmol/L × 24 h. Proportion of cells in G_0-1 or S + G_2-M fractions. *Columns,* mean of triplicate determinations from three independent experiments; *bars,* SD. *P* values show the probability of no difference by *t* test.

Published OnlineFirst January 11, 2007; DOI: 10.1158/1535-7163.MCT-06-0397

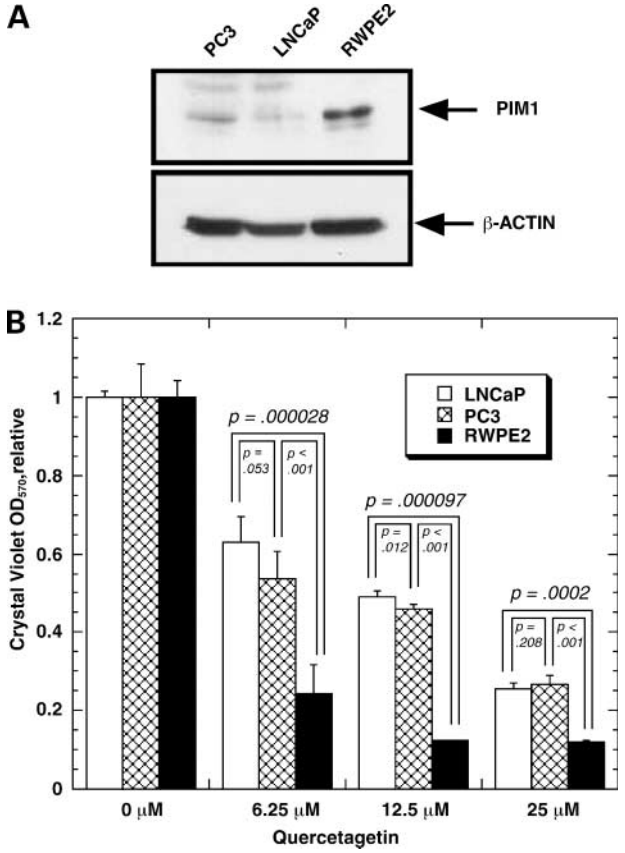

Figure 6. Quercetagetin inhibits the growth of prostate cancer cells in proportion to their content of PIM1. **A,** measurement of intracellular PIM1 in PC3, LNCaP, and RWPE2 prostate cancer cells by immunoblotting. **B,** growth inhibition by treatment of prostate cancer cells with quercetagetin for 72 h. *Columns,* mean of triplicate determinations from one of two similar experiments; *bars,* SD. *P* values were calculated by *t* tests and represent the probability that there is no difference between the two compared populations.

kinases are either less active or less specific flavonoids (7, 9), the same structural class as quercetagetin, or staurosporine analogues (8, 9, 21). We therefore used small interfering RNA as a genetic means to identify a *pim-1*–dependent phenotype. Proliferation of prostate cells was suppressed with both the genetic and chemical inhibitors of PIM1 activity. These data show that quercetagetin is an authentic small-molecule inhibitor of PIM1 kinase.

The crystal structures of PIM1 complexed with quercetagetin, myricetin, and 5,7,3′,4′,5′-pentahydroxyflavonone show that flavonoids bind to PIM1 in two distinct orientations. Although interesting, this is not a surprising observation, as flavones have shown a variety of binding modes in kinases (9, 22, 23, 26–28). An examination of the intermolecular interactions of each flavonoid with PIM1 does not clearly reveal why one orientation was adopted over the other. However, it is possible that the presence of three hydroxyl groups on the B ring of myricetin and 5,7,3′,4′,5′-pentahydroxyflavone discourages these two flavonoids from adopting the binding orientation observed for quercetagetin. The hydrophobic side chain of Leu^{120}, which extends into the ATP pocket in the same region occupied by the B ring of quercetagetin (Fig. 3A), may be incompatible with the 5′ hydroxyl group of myricetin and 5,7,3′,4′,5′-pentahydroxyflavone.

Both *pim-1* and *pim-2* can phosphorylate 4EBP-1, a regulator of protein translation (31, 32). Rapamycin was unable to block this effect. These data suggest that *pim* kinases may function in a parallel pathway to the phosphatidylinositol 3-kinase/AKT/mammalian target of rapamycin cascade to regulate and support protein synthesis under stress conditions. Because AKT-1 and PIM2 function cooperatively to induce lymphoma formation in transgenic mice (6), it may be necessary to target both pathways for effective antitumor effects. Several prototype AKT inhibitors have been described (33, 34). Our identification of quercetagetin as a PIM1 inhibitor provides a tool for tissue culture studies to investigate this hypothesis. Under the tested conditions, we found no evidence that quercetagetin inhibited the phosphorylation of AKT on Ser^{473}. Thus, it may be possible to combine inhibitors of these kinases to detect additive or synergistic effects resulting from the blockade of the two kinase pathways.

References

1. Wang Z, Bhattacharya N, Weaver M, et al. PIM1: a serine/threonine kinase with a role in cell survival, proliferation, differentiation, and tumorigenesis. J Vet Sci 2001;2:167–79.
2. Qian KC, Wang L, Hickey ER, et al. Structural basis of constitutive activity and a unique nucleotide binding mode of human PIM1 kinase. J Biol Chem 2005;280:6130–7.
3. Lilly M, Kraft A. Enforced expression of the Mr 33,000 PIM1 kinase enhances factor-independent survival and inhibits apoptosis in murine myeloid cells. Cancer Res 1997;57:5348–55.
4. Pircher TJ, Zhao S, Geiger JN, Joneja B, Wojchowski DM. PIM1 kinase protects hematopoietic FDC cells from genotoxin-induced death. Oncogene 2000;19:3684–92.
5. Lilly M, Sandholm J, Cooper JJ, Koskinen PJ, Kraft A. The PIM1 serine kinase prolongs survival and inhibits apoptosis- related mitochondrial dysfunction in part through a bcl-2-dependent pathway. Oncogene 1999; 18:4022–31.
6. Hammerman PS, Fox CJ, Birnbaum MJ, Thompson CB. Pim and Akt oncogenes are independent regulators of hematopoietic cell growth and survival. Blood 2005;105:4477–83.
7. Jacobs MD, Black J, Futer O, et al. PIM1 ligand-bound structures reveal the mechanism of serine/threonine kinase inhibition by LY294002. J Biol Chem 2005;280:13728–34.
8. Fabian MA, Biggs WH III, Treiber DK, et al. A small molecule-kinase interaction map for clinical kinase inhibitors. Nat Biotechnol 2005;23: 329–36.
9. Bullock AN, Debreczeni JE, Fedorov OY, Nelson A, Marsden BD, Knapp S. Structural basis of inhibitor specificity of the human protooncogene proviral insertion site in Moloney murine leukemia virus (PIM1) kinase. J Med Chem 2005;48:7604–14.
10. Kueng W, Silber E, Eppenberger U. Quantification of cells cultured on 96-well plates. Anal Biochem 1989;182:16–9.
11. Yan B, Zemskova M, Holder S, et al. The PIM-2 kinase phosphorylates BAD on serine 112 and reverses BAD-induced cell death. J Biol Chem 2003;278:45358–67.
12. Aho TL, Sandholm J, Peltola KJ, Mankonen HP, Lilly M, Koskinen PJ. PIM1 kinase promotes inactivation of the pro-apoptotic Bad protein by phosphorylating it on the Ser^{112} gatekeeper site. FEBS Lett 2004;571: 43–9.

Published OnlineFirst January 11, 2007; DOI: 10.1158/1535-7163.MCT-06-0397

13. Kumar A, Mandiyan V, Suzuki Y, et al. Crystal structures of proto-oncogene kinase PIM1: a target of aberrant somatic hypermutations in diffuse large cell lymphoma. J Mol Biol 2005;348:183 – 93.

14. Mayr GW, Windhorst S, Hillemeier K. Antiproliferative plant and synthetic polyphenolics are specific inhibitors of vertebrate inositol-1,4,5-trisphosphate 3-kinases and inositol polyphosphate multikinase. J Biol Chem 2005;280:13229 – 40.

15. Lee LT, Huang YT, Hwang JJ, et al. Blockade of the epidermal growth factor receptor tyrosine kinase activity by quercetin and luteolin leads to growth inhibition and apoptosis of pancreatic tumor cells. Anticancer Res 2002;22:1615 – 27.

16. Chu SC, Hsieh YS, Lin JY. Inhibitory effects of flavonoids on Moloney murine leukemia virus reverse transcriptase activity. J Nat Prod 1992;55: 179 – 83.

17. Plaper A, Golob M, Hafner I, Oblak M, Solmajer T, Jerala R. Characterization of quercetin binding site on DNA gyrase. Biochem Biophys Res Commun 2003;306:530 – 6.

18. Ko WC, Shih CM, Lai YH, Chen JH, Huang HL. Inhibitory effects of flavonoids on phosphodiesterase isozymes from guinea pig and their structure-activity relationships. Biochem Pharmacol 2004;68:2087 – 94.

19. Lu J, Papp LV, Fang J, Rodriguez-Nieto S, Zhivotovsky B, Holmgren A. Inhibition of mammalian thioredoxin reductase by some flavonoids: implications for myricetin and quercetin anticancer activity. Cancer Res 2006;66:4410 – 8.

20. Bullock AN, Debreczeni J, Amos AL, Knapp S, Turk BE. Structure and substrate specificity of the PIM1 kinase. J Biol Chem 2005;280:41675 – 82.

21. Debreczeni JE, Bullock AN, Atilla GE, et al. Ruthenium half-sandwich complexes bound to protein kinase pim-1. Angew Chem Int Ed Engl 2006; 45:1580 – 5.

22. Walker EH, Pacold ME, Perisic O, et al. Structural determinants of phosphoinositide 3-kinase inhibition by wortmannin, LY294002, quercetin, myricetin, and staurosporine. Mol Cell 2000;6:909 – 19.

23. Lu H, Chang DJ, Baratte B, Meijer L, Schulze-Gahmen U. Crystal structure of a human cyclin-dependent kinase 6 complex with a flavonol inhibitor, fisetin. J Med Chem 2005;48:737 – 43.

24. Clark DE, Errington TM, Smith JA, Frierson HF, Jr., Weber MJ, Lannigan DA. The serine/threonine protein kinase, p90 ribosomal S6 kinase, is an important regulator of prostate cancer cell proliferation. Cancer Res 2005;65:3108 – 16.

25. Alessi DR, Cuenda A, Cohen P, Dudley DT, Saltiel AR. PD 098059 is a specific inhibitor of the activation of mitogen-activated protein kinase kinase *in vitro* and *in vivo*. J Biol Chem 1995;270:27489 – 94.

26. De AW, Jr., Mueller-Dieckmann HJ, Schulze-Gahmen U, Worland PJ, Sausville E, Kim SH. Structural basis for specificity and potency of a flavonoid inhibitor of human CDK2, a cell cycle kinase. Proc Natl Acad Sci U S A 1996;93:2735 – 40.

27. Sicheri F, Moarefi I, Kuriyan J. Crystal structure of the Src family tyrosine kinase Hck. Nature 1997;385:602 – 9.

28. De Azevedo WF, Jr., Mueller-Dieckmann HJ, Schulze-Gahmen U, Worland PJ, Sausville E, Kim SH. Structural basis for specificity and potency of a flavonoid inhibitor of human CDK2, a cell cycle kinase. Proc Natl Acad Sci U S A 1996;93:2735 – 40.

29. Davies SP, Reddy H, Caivano M, Cohen P. Specificity and mechanism of action of some commonly used protein kinase inhibitors. Biochem J 2000;351:95 – 105.

30. McGovern SL, Shoichet BK. Kinase inhibitors: not just for kinases anymore. J Med Chem 2003;46:1478 – 83.

31. Fox CJ, Hammerman PS, Thompson CB. The Pim kinases control rapamycin-resistant T cell survival and activation. J Exp Med 2005;201: 259 – 66.

32. Chen WW, Chan DC, Donald C, Lilly MB, Kraft AS. Pim family kinases enhance tumor growth of prostate cancer cells. Mol Cancer Res 2005;3: 443 – 51.

33. Yang L, Dan HC, Sun M, et al. Akt/protein kinase B signaling inhibitor-2, a selective small molecule inhibitor of Akt signaling with antitumor activity in cancer cells overexpressing Akt. Cancer Res 2004; 64:4394 – 9.

34. Barnett SF, Defeo-Jones D, Fu S, et al. Identification and characterization of pleckstrin-homology-domain-dependent and isoenzyme-specific Akt inhibitors. Biochem J 2005;385:399 – 408.

AACR American Association for Cancer Research

Molecular Cancer Therapeutics

Characterization of a potent and selective small-molecule inhibitor of the PIM1 kinase

Sheldon Holder, Marina Zemskova, Chao Zhang, et al.

Mol Cancer Ther 2007;6:163-172. Published OnlineFirst January 11, 2007.